ELSEVIER

Contents lists available at ScienceDirect

Ecological Informatics

journal homepage: www.elsevier.com/locate/ecolinf





Cellphone picture-based, genus-level automated identification of Chagas disease vectors: Effects of picture orientation on the performance of five machine-learning algorithms

Vinícius Lima de Miranda ^{a,b}, Ewerton Pacheco de Souza ^b, Deborah Bambil ^c, Ali Khalighifar ^d, A. Townsend Peterson ^e, Francisco Assis de Oliveira Nascimento ^f, Rodrigo Gurgel-Gonçalves ^{b,*,1}, Fernando Abad-Franch ^{b,g,1}

- ^a Departamento de Zoologia, Instituto de Ciências Biológicas, Universidade de Brasília, Brasília, Distrito Federal, Brazil
- ^b Faculdade de Medicina, Universidade de Brasília, Brasília, Distrito Federal, Brazil
- ^c Departamento de Biologia Celular, Instituto de Ciências Biológicas, Universidade de Brasília, Brasília, Distrito Federal, Brazil
- d Fish, Wildlife, and Conservation Biology Department, Colorado State University, Fort Collins, CO, USA
- e Department of Ecology and Evolutionary Biology and Biodiversity Institute, University of Kansas, Lawrence, KS, USA
- f Departamento de Engenharia Elétrica, Faculdade de Tecnologia, Universidade de Brasília, Brasília, Distrito Federal, Brazil
- g Instituto Leônidas e Maria Deane Fiocruz Amazônia, Manaus, Amazonas, Brazil

ARTICLE INFO

Keywords: Automated identification Machine learning Accuracy Specificity Low-resolution pictures Triatominae

ABSTRACT

Chagas disease (CD) is a public-health concern across Latin America. It is caused by Trypanosoma cruzi, a parasite transmitted by blood-sucking triatomine bugs. Automated identification of triatomine bugs is a potential means to strengthen CD vector surveillance. To be broadly useful, however, automated systems must draw on algorithms capable of correctly identifying bugs from images taken with ordinary cellphone cameras at varying angles or positions. Here, we assess the performance of five machine-learning algorithms at identifying the main CD vector genera (Triatoma, Panstrongylus, and Rhodnius) based on bugs photographed at different angles/positions with a 72-dpi cellphone camera. Each bug (N=730; 13 species) was photographed at nine angles representing three positions; dorsal-flat, dorsal-oblique, and front/back-oblique. We randomly split the 6570-picture database into training (80%) and testing sets (20%), and then trained and tested a convolutional neural network (AlexNet, AN); three boosting-based classifiers (AdaBoost, AB; Gradient Boosting, GB; and Histogram-based Gradient Boosting, HB); and a linear discriminant model (LD). We assessed identification accuracy and specificity with logit-binomial generalized linear mixed models fit in a Bayesian framework. Differences in performance across algorithms were mainly driven by AN's essentially perfect accuracy and specificity, irrespective of picture angle or bug position. HB predicted accuracies ranged from ~0.987 (Panstrongylus, dorsal-oblique) to >0.999 (Triatoma, dorsal-flat). AB accuracy was poor for Rhodnius (~0.224-0.282) and Panstrongylus (~0.664-0.729), but high for Triatoma (~0.988-0.991). For Panstrongylus, LD and GB had predicted accuracies in the \sim 0.970-0.984 range. AB misclassified \sim 57% of Rhodnius and Panstrongylus as Triatoma, whereas specificity ranged from ~ 0.92 to ~ 1.0 for the remaining algorithm-genus combinations. Dorsal-flat pictures appeared to improve algorithm performance slightly, but angle/position effects were overall weak-to-negligible. We conclude that, when high-performance algorithms such as AN are used, the angles or positions at which bugs are photographed seem unlikely to hinder cellphone picture-based automated identification of CD vectors, at least at the genus level. Future research should focus on combining mixed-quality pictures and state-of-the-art algorithms to (i) identify triatomine adults to the species level and (ii) distinguish triatomine nymphs (i.e., immature stages) from adults and from other insects.

Abbreviations: CD, Chagas disease; AN, AlexNet; AB, AdaBoost Multi-Class Adaptive Boosting classifier; GB, Gradient Boosting classifier; HB, Histogram-based Gradient Boosting classifier; LD, linear discriminant model; DALY, Disability-Adjusted Life Year; GLMM, generalized linear mixed model; AICc, Akaike's information criterion corrected for finite samples.

E-mail address: gurgelrg@hotmail.com (R. Gurgel-Gonçalves).

https://doi.org/10.1016/j.ecoinf.2023.102430

Corresponding author.

¹ Equal contribution

1. Introduction

Pathogens transmitted by insects and other arthropods threaten public health globally; in 2019, an estimated ~700,000 people died and \sim 53.2 million disability-adjusted life years (DALYs) were lost owing to diseases caused by insect-borne viruses (dengue, yellow fever, and Zika), bacteria (trachoma), or parasites (onchocerciasis, lymphatic filariasis, leishmaniasis, African trypanosomiasis, and Chagas disease) (GBD, 2019). In Latin America, the highest-burden vector-borne disease is Chagas disease, with recent estimates suggesting that its causative agent, Trypanosoma cruzi, infects 5.5 to 7.3 million people and leads to annual losses of 169,000 to 490,000 DALYs (GBD, 2019; Rojas de Arias et al., 2022). Trypanosoma cruzi is a blood/tissue protozoan parasite that infects a wide range of mammalian hosts, including humans, and can cause severe heart, digestive, and (less frequently) neurological lesions (Jansen and Roque, 2010; Pérez-Molina and Molina, 2018; Prata, 2001). Trypanosoma cruzi is endemic to the Americas, where it is primarily transmitted by a diverse group of blood-sucking true bugs known as triatomines (Lent and Wygodzinsky, 1979; Monteiro et al., 2018).

A critical requirement for effective control and surveillance of vector-borne diseases, including Chagas disease, is accurate vector identification (Monteiro et al., 2018). However, current vectorsurveillance systems are generally weak (and often becoming even weaker) in Latin America and elsewhere, with expertise in diseasevector taxonomy overall declining (e.g., Almeida et al., 2017; Casas et al., 2016; Gurgel-Gonçalves, 2022; Yadon et al., 2006). Weak surveillance systems limit our ability to assess and stratify disease transmission risk, which in turns hampers the planning and deployment of adequate public-health responses (Gürtler and Cecere, 2021; Hashimoto et al., 2015; Yoshioka et al., 2017). Weaker surveillance, moreover, yields progressively lower-quality and sparser vector-occurrence data records (Abad-Franch et al., 2013, 2014). This data gap not only hinders research on how vector distribution patterns change over time or across space; worse still, it can foster the false impression that the vectors themselves, and not just the records of their occurrence, are becoming rarer. This 'low-risk delusion' may self-reinforce via fading priority, funding cuts, even sparser records, and so forth in a perverse, positivefeedback loop (Abad-Franch et al., 2013, 2014; Schofield et al., 2006).

In this context of ever-weakening surveillance systems, researchers and public-health officials have insisted on the need to develop and test new tools and strategies to strengthen Chagas disease vector surveillance (e.g., Abad-Franch et al., 2011, 2014; Dias et al., 2016; Gurgel-Gonçalves, 2022; Gürtler and Cecere, 2021; Schofield et al., 2006; WHO, 2002, 2017). Efforts in that direction have addressed several sides of surveillance, including, e.g., improving vector-detection probabilities (Abad-Franch et al., 2011; Gürtler and Cecere, 2021); promoting instruction in medical entomology (Casas et al., 2016; Gurgel-Gonçalves, 2022); devising entomological-risk scoring/stratification systems that do not rely entirely on actual vector-occurrence records (e.g., Ribeiro-Jr et al., 2021); or developing electronic, easy-to-use vector identification keys (Gurgel-Gonçalves et al., 2021; Oliveira et al., 2017).

An approach that has gained traction in recent years is using machine learning-based systems for the automated identification of triatomine bugs (Abdelghani et al., 2021; Cochero et al., 2022; Cruz et al., 2020, 2021; Gurgel-Gonçalves et al., 2017; Khalighifar et al., 2019; Parsons and Banitaan, 2021). In these systems, machine-learning algorithms are trained, and then tested, on collections of digital pictures featuring bugs of known taxonomic identity. This 'ground-truth' picture set is usually composed of relatively high-quality, standardized digital pictures displaying the full dorsal aspect of the bugs (e.g., Abdelghani et al., 2021; Cruz et al., 2021; Gurgel-Gonçalves et al., 2017; Khalighifar et al., 2019). To be broadly useful, however, automated systems must be capable of correctly identifying bugs photographed with ordinary digital cameras at varying angles or positions – i.e., the kind of information that surveillance staff or citizens in general will likely generate and feed into real-world, 'extended' vector-surveillance systems (Cochero et al., 2022;

see also, e.g., Motta et al., 2019; Park et al., 2020; Terry et al., 2020; Justen et al., 2021; Pataki et al., 2021).

Here, we assess the performance of five machine-learning algorithms at identifying Chagas disease vectors based on bugs photographed at different angles or positions with an ordinary cellphone camera. Our assessment of algorithm performance builds upon statistical models that formally account for the non-independence of results (i.e., correct vs. incorrect identifications) stemming from the same individual picture, from pictures featuring the same individual specimen, and from (pseudo-)replicate training-testing runs in which all algorithms used the same training and testing picture sets (see below). As such, model-based algorithm performance estimates and their associated measures of uncertainty take data dependencies into account (Bolker et al., 2009; Harrison et al., 2018; see also Gurgel-Gonçalves et al., 2021). Although we built a unique collection of 6570 digital pictures of 730 individual specimens, our species-level coverage was still limited; therefore, we focus on algorithm performance at the genus level, for which we were able to gather large enough samples of specimens and pictures. We follow the currently accepted systematic arrangement for the Triatominae (Monteiro et al., 2018), with all our bugs falling into one of the three genera to which the main vectors of human Chagas disease, from the USA to Argentina, all belong – Triatoma, Panstrongylus, and Rhodnius (WHO, 2002). Our assessment shows that convolutional neural networks can identify these major triatomine genera with very high accuracy using low-resolution pictures taken with ordinary cellphone cameras, irrespective of the angles or positions at which the bugs were photographed. This result paves the way for 'hybrid' entomological surveillance systems combining human taxonomic expertise with machine learning-based, automated vector identification.

2. Methods

2.1. Bug-picture database

We worked with a sample of 730 adult, dried, pinned triatomines belonging to 13 species within three genera: Triatoma (400 specimens), Panstrongylus (110 specimens), and Rhodnius (220 specimens) (Table 1). RG-G and VLdM completed 'ground-truth' species-level identifications using printed keys and descriptions (Lent and Wygodzinsky, 1979; Galvão, 2014), the electronic TriatoDex key (Gurgel-Gonçalves et al., 2021), and information on the geographic origin of the specimens. After removing the entomological pin, we placed each bug on a white, rotating circular base and photographed it nine times, one at each of nine different angles representing three positions - dorsal-flat, dorsaloblique, and front/back-oblique (Fig. 1). All pictures were taken using the same Moto G6 Play cellphone (Motorola Mobility LLC, Chicago, IL), which was mounted on a tripod and positioned above the bug as shown in Fig. 1; we used neither the flash nor the zoom functions of the cellphone camera. We saved the pictures in red-green-blue (RGB) format at 72-dpi resolution, and cropped them to a square format (see Fig. 1). Overall, our dataset thus includes 6570 unique pictures featuring 730 individual bugs (Table 1). The pictures are available on figshare (Miranda et al., 2023), and the full raw dataset, including picture metadata, is provided in Supplementary Dataset S1.

2.2. Algorithms

We used five machine-learning algorithms based on three different principles: a pre-trained convolutional neural network (AlexNet); three boosting-based classifiers (AdaBoost Adaptive Boosting, Gradient Boosting, and Histogram-based Gradient Boosting); and a linear discriminant model. Here, we briefly describe the characteristics of these algorithms and the inputs that they require; further details can be found in the references provided below.

The architecture of AlexNet ('AN' hereafter), which includes five convolutional layers and three fully-connected layers, has 60 million

Table 1Cellphone picture-based automated identification of Chagas disease vectors: summary of triatomine bugs and pictures used in the study.

Genus	Species	Bug p	Bug position in picture*			
		A	В	С		
Triatoma	Triatoma brasiliensis	130	780	260	1170	
	Triatoma costalimai	40	240	80	360	
	Triatoma infestans	60	360	120	540	
	Triatoma lenti	40	240	80	360	
	Triatoma melanocephala	20	120	40	180	
	Triatoma rubrovaria	30	180	60	270	
	Triatoma sherlocki	30	180	60	270	
	Triatoma sordida	30	180	60	270	
	Triatoma vitticeps	20	120	40	180	
	Subtotal	400	2400	800	3600	
Panstrongylus	Panstrongylus lutzi	20	120	40	180	
	Panstrongylus megistus	90	540	180	810	
	Subtotal	110	660	220	990	
Rhodnius	Rhodnius neglectus	200	1200	400	1800	
	Rhodnius pictipes	20	120	40	180	
	Subtotal	220	1320	440	1980	
Grand total		730	4380	1460	6570	

^{*} Bugs were photographed at nine angles representing three positions: dorsal-flat (**A**; one picture per bug, so that figures in this column also indicate the number of unique specimens in each class); dorsal-oblique (**B**; six pictures per bug); and front/back-oblique (**C**; two pictures per bug); see Fig. 1.

parameters; AN uses RGB images, 227×227 pixels in size, as input. AN was pre-trained on 1.2 million images of varying resolution and representing 1000 classes (i.e., different objects, animals, plants, etc.) from the ImageNet database (Krizhevsky et al., 2012). We note that, although AN is more complex than the other algorithms that we tested (see below), much of its extra computational cost is associated with pre-training on ImageNet data.

We also tested four 'classical' machine-learning algorithms: Ada-Boost Multi-Class Adaptive Boosting ('AB' hereafter), Gradient Boosting ('GB' hereafter), Histogram-based Gradient Boosting ('HB' hereafter), and a linear discriminant model ('LD' hereafter). Instead of directly taking pictures as input, these algorithms use numerical 'features' extracted from, and representing attributes of, those pictures. We used *Inovtaxon* (Bambil et al., 2020) to extract 226 picture features (namely, 36 colour features, 135 shape features, and 55 texture features) that were used as input to feed the algorithms (see Bambil et al., 2020 and htt ps://github.com/DeborahBambil/Inovtaxon for details; see also Hu, 1962; Zhao and Pietikainen, 2007; Flusser et al., 2009; Deniz et al., 2011; Nascimento et al., 2023).

AB combines multiple weak classifiers into a strong classifier capable of handling multi-class problems; at each training iteration, AB uses weights to 'tag' misidentified samples so that later iterations can 'learn' these mistakes, thus improving overall accuracy (Freund and Schapire, 1997). GB sequentially combines multiple decision trees, with iterative adjustment ('learning') based on the residual errors of previous models and minimization based on gradient descent (Friedman, 2001). HB is a fast, computationally efficient approach to gradient boosting in which continuous input variables ('features') are discretized into bins and then arranged as histograms; model training is thus much faster and memory efficient, allowing the use of gradient boosting with large datasets (Dalal and Triggs, 2005). Finally, LD is a classical dimension-reduction procedure in which linear functions of input values are computed that maximize among-class relative to within-class variance, thus maximizing class discrimination (Fisher, 1936). In the context of machine learning, these 'linear discriminant functions' are computed during training and then used to assign test instances to their most likely class (Tharwat et al., 2017).

2.3. Algorithm training and testing

We trained all algorithms on a random subset of 5256 pictures (80%

of the 6570-picture dataset). To gauge performance consistency, the training-testing process was repeated 10 times for each algorithm; in each of these (pseudo-)replicate runs, all five algorithms used the same training and testing picture subsets.

AN was implemented in MATLAB (www.mathworks.com). For training, we used the stochastic gradient descent with momentum optimizer with default settings except for the initial learning rate (which we set to 0.001) and the maximum number of epochs (which we set to 15 after preliminary tests). The 'classical' machine-learning algorithms (AB, GB, HB, and LD) were run in Python (www.python.org) using the *scikit-learn* toolbox (Pedregosa et al., 2011). We left hyperparameters at *scikit-learn* default values, except for the learning rate of GB and HB (which we set to 0.15) and the tolerance threshold value for LD (set to 1×10^{-5}).

In each of the 10 (pseudo-)replicate runs, all algorithms were tested on the same subset of 1314 'problem pictures' – for each of which we scored whether the class label predicted by the algorithm did or did not match the 'ground-truth' label. These correct or incorrect binary predictions were used as outcome variables in downstream analyses.

2.4. Data analysis: assessing algorithm performance

We analyzed the outcome of our 50 testing runs (10 per algorithm) using R 4.2.1 (R Core Team, 2022) and the RStudio 2023.03.1.446 interface (Posit Software, 2022). We first summarized our data in descriptive tables, including cross-classification or 'confusion' matrices, calculated Cohen's κ agreement scores (Cohen, 1960), and ran simple exploratory analyses by calculating and graphing frequencies and proportions. Proportions and their Wilson 'score' 95% confidence intervals (CIs) (Newcombe, 1998) were computed using the *Hmisc* R package (Harrel and Dupont, 2023).

Next, we used generalized linear mixed models (GLMMs; Bolker et al., 2009; Harrison et al., 2018) with binomial error distribution and logit link-function to investigate (i) whether and to what extent two key identification-performance metrics, accuracy and specificity, varied across algorithms ('algorithm' predictor, a five-level factor) and bug genera ('genus' predictor, a three-level factor); and (ii) the effects of cellphone-picture characteristics (picture 'angle', a nine-level factor; or bug 'position', a three-level factor; see Fig. 1) on algorithm performance. Covariates 'angle' and 'position', which are correlated by construction, did not appear together in any model. Initially, all models included a 'picture-within-bug' nested random effect to account for the nonindependence of results arising from the same picture and from pictures of the same specimen. In some cases, however, this model specification led to convergence issues, so the models were simplified (see Specificity below). Because in each (pseudo-)replicate run all algorithms ran on the same data (i.e., picture) subsets, we also included a 'replicate' random effect in the models.

We fit our GLMMs in a Bayesian framework using the *blme* R package, with weak, normal ($\mu=0$, $\sigma^2=9$) fixed-effect priors and flat covariance priors (Bolker, 2018; Chung et al., 2013, 2015; Dorie et al., 2022). Relative model performance was evaluated based on sample-size corrected Akaike's information criterion (AICc) scores and related metrics (Burnham and Anderson, 2002) computed with the *bbmle* R package (Bolker et al., 2022). AICc calculations used the number of unique specimens in each dataset/subset (see below) as the sample size. For inference, we focused on the top-ranking (smallest-AICc) model in each model set (accuracy plus genus-specific specificity; see below) (Burnham and Anderson, 2002).

Accuracy. Accuracy analyses made use of the full, 65,700-observation dataset. The binary dependent variable specified whether each picture was (coded 1) or was not (coded 0) correctly identified in each identification task. Note that stratification by genus (i.e., inclusion of the 'genus' fixed effect in a model) implies conditioning on bug genus, so that genus-specific accuracy estimates can be interpreted as estimates of sensitivity, defined as the probability of getting a correct answer,

conditioned on genus identity. We fitted (1) an intercept-only model; (2) four bivariate models, each including one of the variables of interest ('algorithm'; bug 'genus'; picture 'angle'; bug 'position'); (3) five additive models including 'algorithm' and combinations of the other predictors; and (4) five interaction models including 'algorithm \times genus'; 'algorithm \times position'; and 'genus \times position' interaction terms (see Table 2). We initially also considered (i) two-way interactions involving the nine-level 'angle' covariate, and (ii) three-way ('algorithm \times genus \times position') interactions; these highly complex models, however, often showed signs of convergence issues, and we did not consider them further.

Specificity. For a given bug genus, specificity analyses were based on the subset of data corresponding to bugs not belonging in that genus. The binary dependent variable specified whether the bug in each picture was (coded 1) or was not (coded 0) correctly identified as not belonging in the focal genus, conditional on the picture featuring a bug indeed not belonging in that genus. Some of the specificity models had clear signs of convergence issues, most likely because correct-identification frequencies were high across data subsets and, within them, across strata. We therefore simplified the structure of our specificity models by dropping the 'angle' fixed effect, interaction terms, and the 'picturewithin-bug' random effect. Note that this simplification means that (i) subtler patterns of variation in specificity may exist that our models do not capture, and (ii) uncertainty around model coefficients (and, hence, around model predictions) may be underestimated. For each genus, the specificity-analysis model set thus included (1) an intercept-only model; (2) three bivariate models ('algorithm'; 'genus'; bug 'position'); and (3) three additive models ('algorithm' + 'genus'; 'algorithm' + 'position'; and 'algorithm' + 'genus' + 'position') (see Table 3).

3. Results

3.1. Accuracy

Fig. 2 summarizes the main results of the full set of 50 testing runs. The pre-trained convolutional neural network, AN, correctly identified the genus of the specimen featured in every one of the 5896 unique pictures on which it was tested across the 10 (pseudo-)replicate runs. In contrast, AB overall accuracy was only \sim 0.692, with (pseudo-)replicate run-specific values ranging from 0.595 to 0.760. Accuracy was high (\sim 0.976 overall) for HB, and was also above 95% for GB (\sim 0.965) and LD (~0.959); variation across (pseudo-)replicate runs was small for these three algorithms (Fig. 2). On average, genus-level identification was more accurate for pictures featuring Triatoma specimens (observed sensitivity 0.967) than for those featuring bugs in *Panstrongylus* (0.855) or Rhodnius (0.918) (Fig. 2). Finally, overall accuracy did not change much across picture angles or bug positions (Fig. 2). Detailed numerical results for these exploratory analyses of observed accuracy are provided in Supplementary Tables S1-S6, and the full raw data are available in Supplementary Dataset S1.

In Fig. 3, we present a set of confusion matrices summarizing patterns of correct and incorrect identification of bug pictures across algorithms and genera and over the 10 (pseudo-)replicate runs that each algorithm completed. AB had a strong tendency to misidentify *Rhodnius*

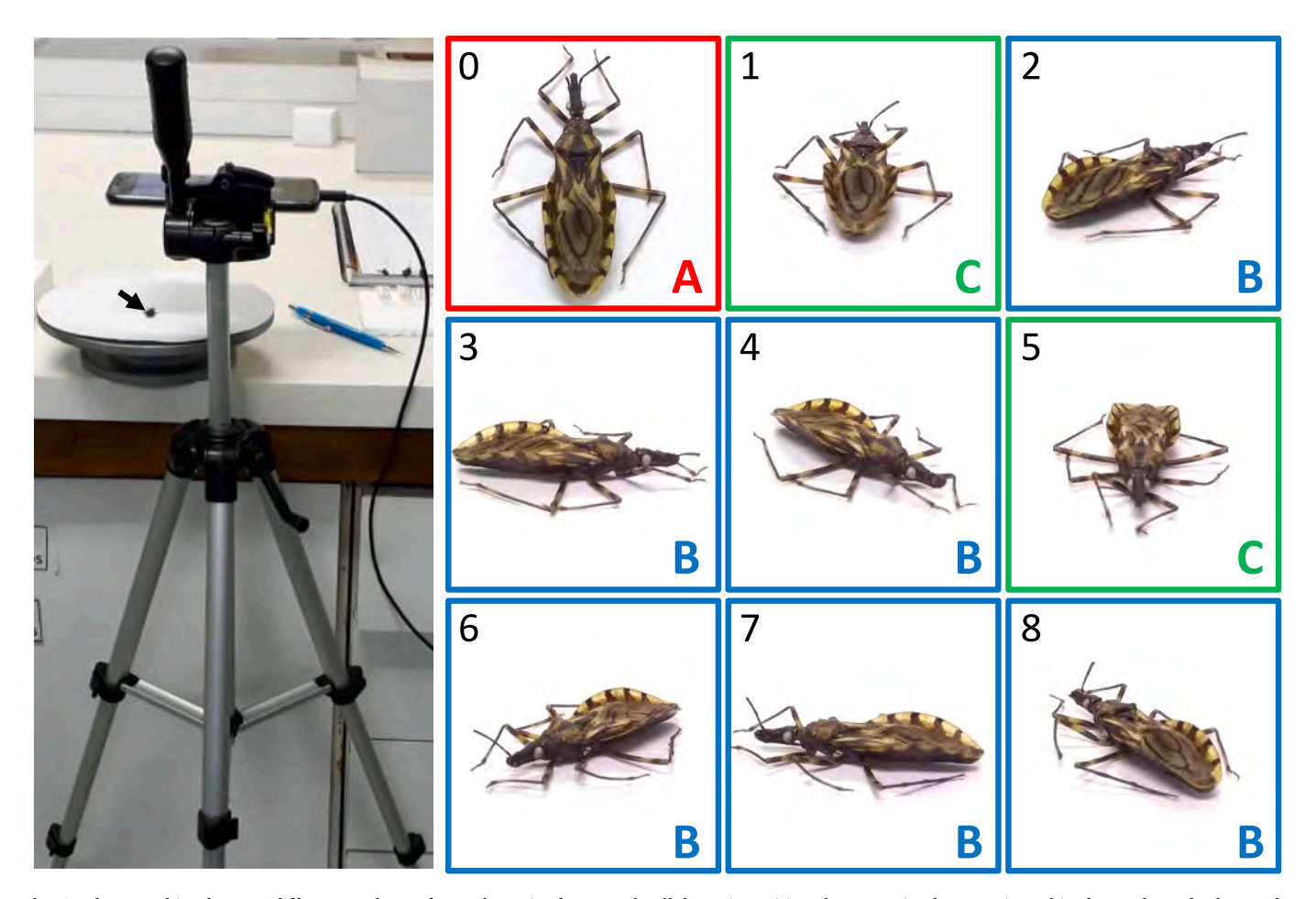


Fig. 1. Photographing bugs at different angles. Left panel: a tripod-mounted cellphone is positioned over a circular, rotating white base where the bug to be photographed (arrow) is placed. Right panels: each bug (here, a *Triatoma brasiliensis* specimen) was photographed at nine angles (0–8) representing three positions (colored letters and picture outlines): A-red, dorsal-flat (picture 0); B-blue, dorsal-oblique (pictures 2–4 and 6–8); and C-green, front/back-oblique (pictures 1 and 5). (For interpretation of the references to colour in this figure legend, the reader is referred to the web version of this article.)

 Table 2

 Accuracy model set. All models included a picture-within-bug nested random effect and a (pseudo-)replicate run random effect.

Model	AICc	ΔAICc	k	Weight	Terms (fixed effects)			
					Algorithm	Genus	Angle	Position
A×G+P	17246.0	0.0	20	0.87	×	×		
$A \times G$	17249.8	3.8	18	0.13	×	×		
$A+G\times P$	18783.0	1537.0	16	< 0.001		×		×
A+G+P	18783.3	1537.3	12	< 0.001				
A+G+An	18786.1	1540.1	18	< 0.001				
A+G	18786.5	1540.5	10	< 0.001				ı
$A \times P + G$	18787.6	1541.6	20	< 0.001	×			×
A+P	19260.6	2014.6	10	< 0.001			ı	
A+An	19262.7	2016.7	16	< 0.001				
A	19263.7	2017.7	8	< 0.001				ı
$A \times P$	19264.3	2018.3	18	< 0.001	×			×
G	31412.3	14166.3	6	< 0.001				
P	31862.4	14616.4	6	< 0.001			ı	
Null	31864.7	14618.7	4	< 0.001				
An	31865.2	14619.2	12	< 0.001				

AICc, sample size-corrected Akaike's information criterion; Δ AICc, AICc difference with the top-ranking (lowest-AICc) model; k, number of parameters; Weight, Akaike weight.

Shaded cells indicate that the term was included (as a fixed effect) in the model; the 'x' symbol indicates which terms are involved in an interaction.

 Table 3

 Specificity model sets. All models included a (pseudo-)replicate random effect. Note that there is one model set for each genus.

Genus	Model	AICc	ΔAICc	k	Weight	Terms (fixed effects)		
						Algorithm	Genus	Position
Triatoma	T A+G+P	14221.9	0.0	9	0.529			
	TA+G	14223.7	1.8	7	0.220			
	T A+P	14224.1	2.2	8	0.177			
	ΤA	14225.8	3.9	6	0.074			
	T G	23904.8	9682.9	3	< 0.001			
	T Null	23905.3	9683.4	2	< 0.001			
	ΤP	23905.8	9683.9	4	< 0.001			
Panstrongylus	PA+G+P	7592.5	0.0	9	0.830			
	PA+G	7595.8	3.2	7	0.170			
	PA+P	8477.6	885.1	8	< 0.001			
	PA	8482.1	889.6	6	< 0.001			
	P G	8778.5	1186.0	3	< 0.001			
	PΡ	9643.5	2051.0	4	< 0.001			
	P Null	9647.8	2055.3	2	< 0.001			
Rhodnius	R A+G+P	2327.2	0.0	9	0.992			
	RA+G	2336.9	9.7	7	0.008			
	R A+P	2419.6	92.4	8	< 0.001			
	R G	2429.1	101.9	3	< 0.001			
	R A	2429.4	102.2	6	< 0.001			
	R P	2511.5	184.3	4	< 0.001			
	R Null	2521.5	194.3	2	< 0.001			

AICc, sample size-corrected Akaike's information criterion; Δ AICc, AICc difference with the top-ranking (lowest-AICc) model; k, number of parameters; Weight, Akaike weight.

Shaded cells indicate that the term was included (as a fixed effect) in the model; all models are additive.

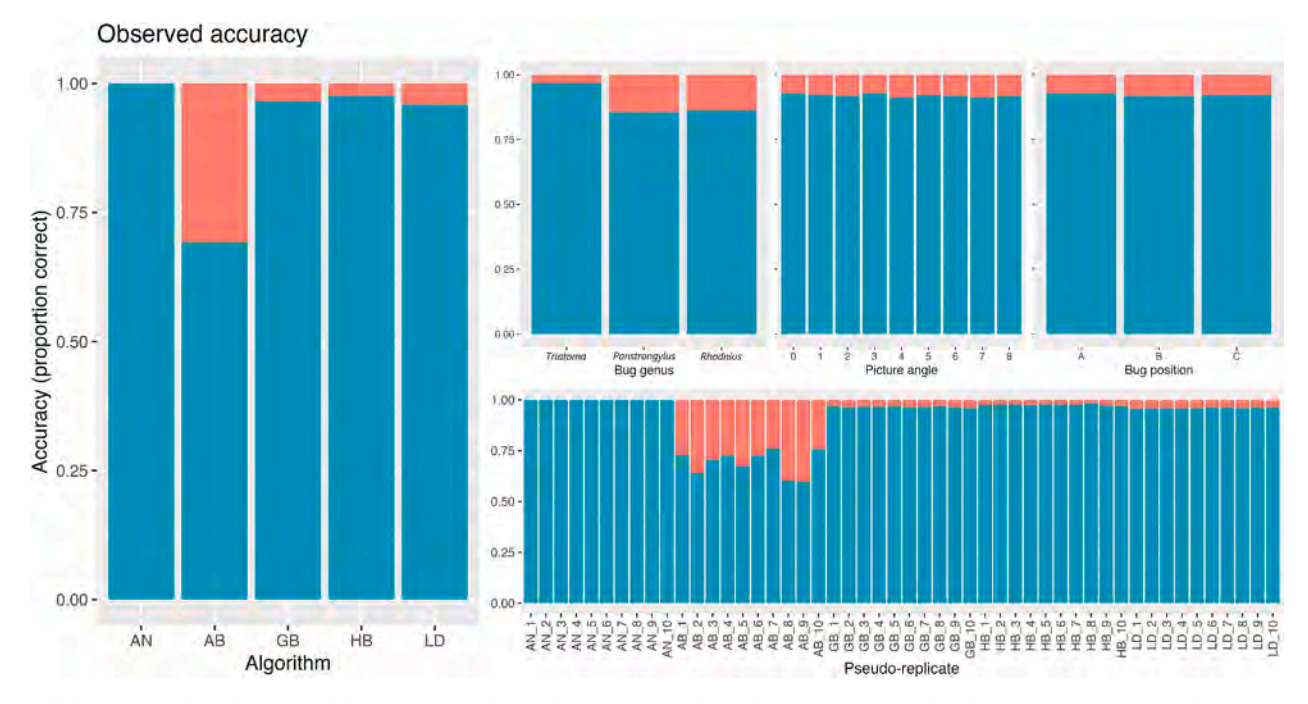


Fig. 2. Cellphone picture-based automated identification of Chagas disease vectors: observed accuracy, measured as the proportion of pictures that were correctly identified (blue bars) to the genus level. Left: results by algorithm (AN, AlexNet; AB, AdaBoost Adaptive Boosting; GB, Gradient Boosting; HB, Histogram-based Gradient Boosting; and LD, linear discriminant model). Right top: results stratified by (i) triatomine bug genus (i.e., the probability of correct identification, conditioned on genus, which can be interpreted as sensitivity); (ii) the nine angles at which bugs were photographed (see Fig. 1); and (iii) bug position (A, dorsal-flat; B, dorsal-oblique; C, front/back-oblique; see Fig. 1). Bottom right: results for each of the 10 (pseudo-)replicate runs completed by each algorithm. The data underlying these graphs, along with score 95% confidence intervals for each proportion, are provided in Supplementary Tables S1–S5. (For interpretation of the references to colour in this figure legend, the reader is referred to the web version of this article.)

as *Triatoma*, and confusion between *Triatoma* and *Panstrongylus* was also evident. Although GB, HB, and especially LD also struggled somewhat to tell *Triatoma* from *Panstrongylus*, they did so to a much lesser extent than AB. On the other hand, we found no instances of confusion between *Panstrongylus* and *Rhodnius* (Fig. 3).

The top-performing accuracy GLMM had strong relative support from the data, with an AICc score 3.8 units smaller than that of the second-ranking model and an Akaike weight of 0.87 (Table 2). This topranking model includes an 'algorithm \times genus' interaction term and an additive bug 'position' term as fixed effects. In Fig. 4, we provide a plot of model predictions for each genus, algorithm, and bug position (see Supplementary Table S7 for numerical model output). The model captures the essentially perfect accuracy of AN, and suggests that variation across algorithms was contingent on bug genus - with, e.g., AB performing fairly well with Triatoma, yet poorly with Rhodnius and Panstrongylus, and both GB and LD struggling somewhat with Panstrongylus (Fig. 4, Supplementary Table S7). In contrast, bug position effects were minor; if anything, dorsal-flat pictures improved accuracy, albeit only slightly, relative to dorsal-oblique pictures (Fig. 4). The top-ranking model estimated a much smaller random-effect variance for the (pseudo-)replicate grouping factor ($\sigma^2 = 0.065$) than for the specimen $(\sigma^2 = 3.683)$ or picture $(\sigma^2 = 2.546)$ grouping factors (Supplementary Table S7). The second-ranking model (Akaike weight = 0.13; Table 2) did not include the bug 'position' covariate - whose effect, therefore, this model estimated as effectively zero. Other models, including the 'null' model, had no support from the data (Table 2). We finally note that models including the nine-level 'angle' covariate performed consistently worse (i.e., had larger AICc scores) than their counterparts including the simpler, four-level 'position' covariate (Table 2). In line with the stratification-by-angle results shown in Fig. 2 and Supplementary Table S3, this result suggests that picture angle had negligible effects on accuracy.

3.2. Specificity

Specificity measures the complement of the false-positive rate, providing insight into misclassification probabilities. As noted above, AN consistently identified all bugs in their correct genus, so specificity was also essentially perfect (Fig. 5; see also Fig. 3). On the other extreme, most of the bugs identified as 'Triatoma' by AB were not Triatoma, yielding a low observed specificity of ~0.431 (Fig. 5; see also Fig. 3 and Supplementary Table S9). Identifications of 'Triatoma' by GB, HB, and LD were overall more reliable, yet observed specificities were modest, from ~0.945 for LD to ~0.965 for HB (Figs. 3 and 5; Supplementary Table S9). Except for AB (observed specificity ~0.944), non-Panstrongylus bugs were rarely confused with Panstrongylus by the remaining algorithms (Figs. 3 and 5). Finally, only a small fraction of pictures featuring non-Rhodnius bugs were misidentified as featuring a Rhodnius specimen, with specificities consistently above 99% (Figs. 3 and 5; Supplementary Table S9).

Table 3 summarizes the structure and relative performance of the seven models in each of the three model sets we fit to assess specificity. In all cases, the top-ranking model was the 'full' additive model including the three covariates we considered ('algorithm', 'genus', and 'position'), and all data-supported models consistently included the 'algorithm' covariate (Table 3). For Triatoma, the second- and thirdranking models had also some support from the data (Table 3); they differed from the top-ranking model in that they lacked, respectively, the 'position' and 'genus' covariates, suggesting that their effects were likely small. The numerical output of the top-ranking model confirmed this, with absolute values of coefficient estimates ranging from 0.096 to 0.168 (Supplementary Table S10). Similarly, the second-ranking Panstrongylus specificity model lacked the 'position' covariate, again indicating that it had, if anything, small effects; in the top-ranking model, the coefficients were small and their 95% CIs included 0 (see Table 3 and Supplementary Table S11). In contrast, the top-ranking Rhodnius model

AlexNet (AN; κ = 1.00)						
		Triatoma	Panstrongylus	Rhodnius	Sum	
	Triatoma	7193	0	0	7193	
Truth	Panstrongylus	0	1986	0	1986	
	Rhodnius	0	0	3961	3961	
Sum		7193	1986	3961	13,140	
AdaBoost			13.5			
(AB; K = 0	.42)	Triatoma	Triatoma Panstrongylus Rho		Sum	
N. A.	Triatoma	6522	628	43	7193	
Truth	Panstrongylus	806	1180	0	1986	
	Rhodnius	2577	0	1384	3961	
Sum	-	9905	1808	1427	13,140	
Gradient-	based Boosting		Prediction		F-1	
(GB; κ = 0.94)		Triatoma	Panstrongylus	Rhodnius	Sum	
Truth	Triatoma	7008	110	75	7193	
	Panstrongylus	216	1770	0	1986	
	Rhodnius	61	0	3900	3961	
Sum		7285	1880	3975	13,140	
Histogram-based Boosting			1200			
(HB; κ = 0.96)		Triatoma	Panstrongylus	Rhodnius	Sum	
	Triatoma	7086	68	39	7193	
Truth	Panstrongylus	165	1821	0	1986	
. 4	Rhodnius	43	0	3918	3961	
Sum		7294	1889	3957	13,140	
Linear Discriminant model (LD; κ = 0.93)			- 27			
		Triatoma	Panstrongylus	Rhodnius	Sum	
Truth	Triatoma	6982	173	38	7193	
	Panstrongylus	256	1730	0	1986	
	Rhodnius	73	0	3888	3961	
Sum		7311	1903	3926	13,140	

Fig. 3. Cellphone picture-based automated identification of Chagas disease vectors: confusion (cross-classification) matrices across algorithms (with Cohen's k agreement scores) and bug genera. The numbers of pictures correctly and incorrectly identified at the genus level are in blue and red cells, respectively. Note that, for each algorithm, the results arise from 10 (pseudo-)replicate runs; in each run, all algorithms were trained and tested on the same picture subsets, which were randomly drawn from the full 6570-picture dataset. (For interpretation of the references to colour in this figure legend, the reader is referred to the web version of this article.)

was strongly supported (Akaike weight =0.99; Table 3), and its numerical output suggested a clearer negative effect of dorsal-oblique pictures on specificity ($\beta_{Position\ B}=-0.594,$ SE 0.277; Supplementary Table S12).

In Fig. 6, we present the predictions of the three top-ranking specificity models. The graphs highlight (i) the essentially perfect performance of AN; (ii) the poor performance of AB with non-*Triatoma* bug pictures; and (iii) the overall high to very high, often close to 100%, specificity of all algorithms with non-*Panstrongylus* and non-*Rhodnius* bugs (Fig. 6; see also Supplementary Tables S13– S15). We note, however, that these models did not include picture or specimen random effects (which led to convergence issues); in interpreting model-based estimates and predictions, therefore, it is important to keep in mind that their associated measures of uncertainty may be smaller than they should be.

4. Discussion

In this study we show that deep-learning algorithms can use low-resolution pictures taken at varying angles with ordinary cellphone

cameras to identify Chagas disease vectors reliably at the genus level. This key result brings us a step closer to the broader aim of developing automated vector-identification tools that, by leveraging information from potentially large, geographically diffuse networks of cellphone users (including vector control-surveillance staff and citizens in general), can help to strengthen real-world vector-surveillance systems in the present context of dwindling taxonomic expertise (Gurgel-Goncalves, 2022). More generally, our results contribute to continuing efforts towards structuring 'extended' surveillance systems in which classical and novel approaches to vector detection, identification, reporting, and mapping can be integrated into more effective, flexible tools for risk assessment and decision-making (e.g., Abad-Franch, 2016; Abad-Franch et al., 2009, 2011, 2013, 2014; Abdelghani et al., 2021; Bender et al., 2020; Ceccarelli et al., 2018, 2020, 2022; Cochero et al., 2022; Cruz et al., 2020, 2021; Curtis-Robles et al., 2015; Delgado-Noguera et al., 2022; Gorla, 2002; Gurgel-Gonçalves et al., 2012, 2017, 2021; Gürtler and Cecere, 2021; Hamer et al., 2018; Khalighifar et al., 2019; Leite et al., 2011; Marsden, 1984; Oliveira et al., 2017; Parsons and Banitaan, 2021; Ribeiro-Jr et al., 2021; Silveira et al., 1984; Vinhaes et al., 2014).

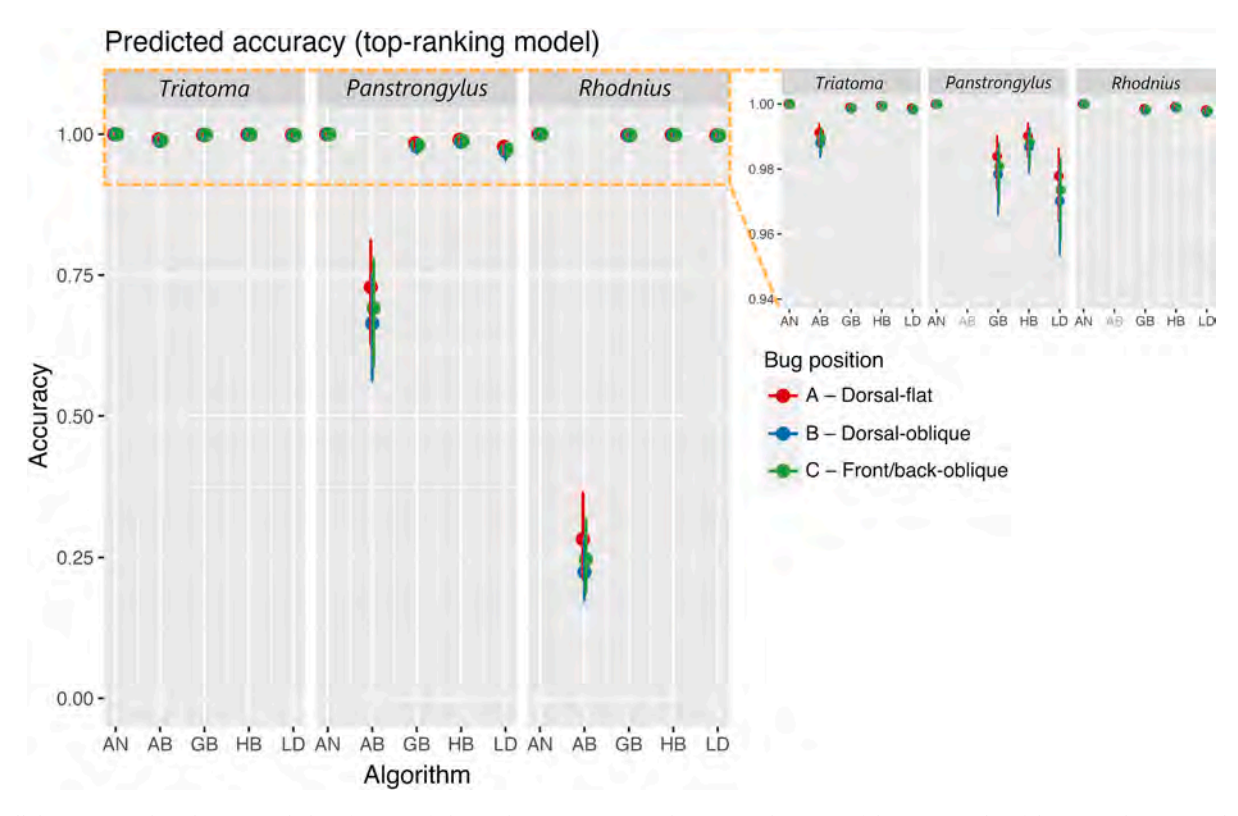


Fig. 4. Cellphone picture-based automated identification of Chagas disease vectors: predictions (with 95% confidence intervals) of the top-ranking generalized linear mixed model for accuracy (see Table 2 and Supplementary Table S7). Accuracy predictions are presented for five algorithms (AN, AlexNet; AB, AdaBoost Adaptive Boosting; GB, Gradient Boosting; HB Histogram-based Gradient Boosting; and LD, linear discriminant model), three triatomine-bug genera (*Triatoma, Panstrongylus*, and *Rhodnius*), and three bug positions (see legend and Fig. 1). The top-right panel is a zoom-in view of the region highlighted by a dashed-orange box in the main graph. The data underlying this figure are provided in Supplementary Table S8.

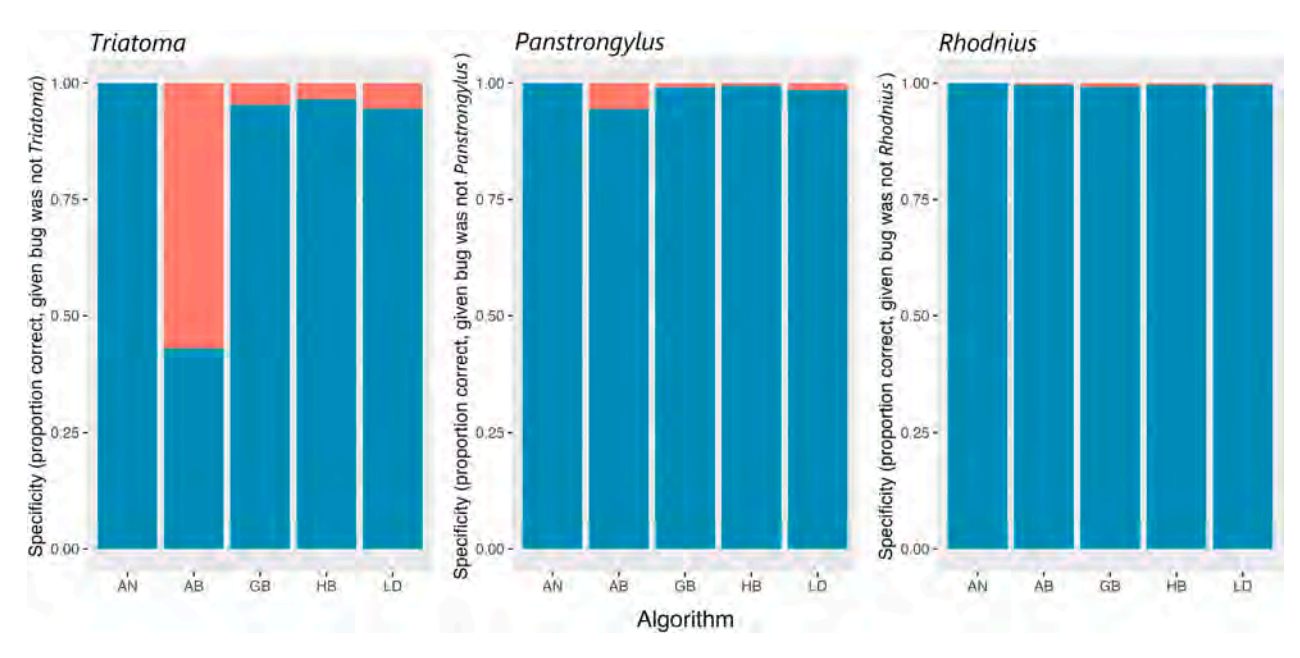


Fig. 5. Cellphone picture-based automated identification of Chagas disease vectors: observed specificity, measured as the proportion of pictures that were correctly identified (blue bars) as *not* belonging in the genus given above each graph. Note that, in this case, red bars represent the false-positive rate. For each genus, results were stratified by algorithm (AN, AlexNet; AB, AdaBoost Adaptive Boosting; GB, Gradient Boosting; HB, Histogram-based Gradient Boosting; and LD, linear discriminant model). The data underlying these graphs, along with score 95% confidence intervals for each proportion, are provided in Supplementary Table S9. (For interpretation of the references to colour in this figure legend, the reader is referred to the web version of this article.)

Our comparative assessment singled out the pre-trained, convolutional neural network, AlexNet (Krizhevsky et al., 2012), as clearly the best-performing algorithm among the five we tested (Figs. 2–6). This

result is in line with previous work showing that artificial neural networks can accurately identify disease vectors (Cochero et al., 2022; Motta et al., 2019; Park et al., 2020; Pataki et al., 2021) and other insects

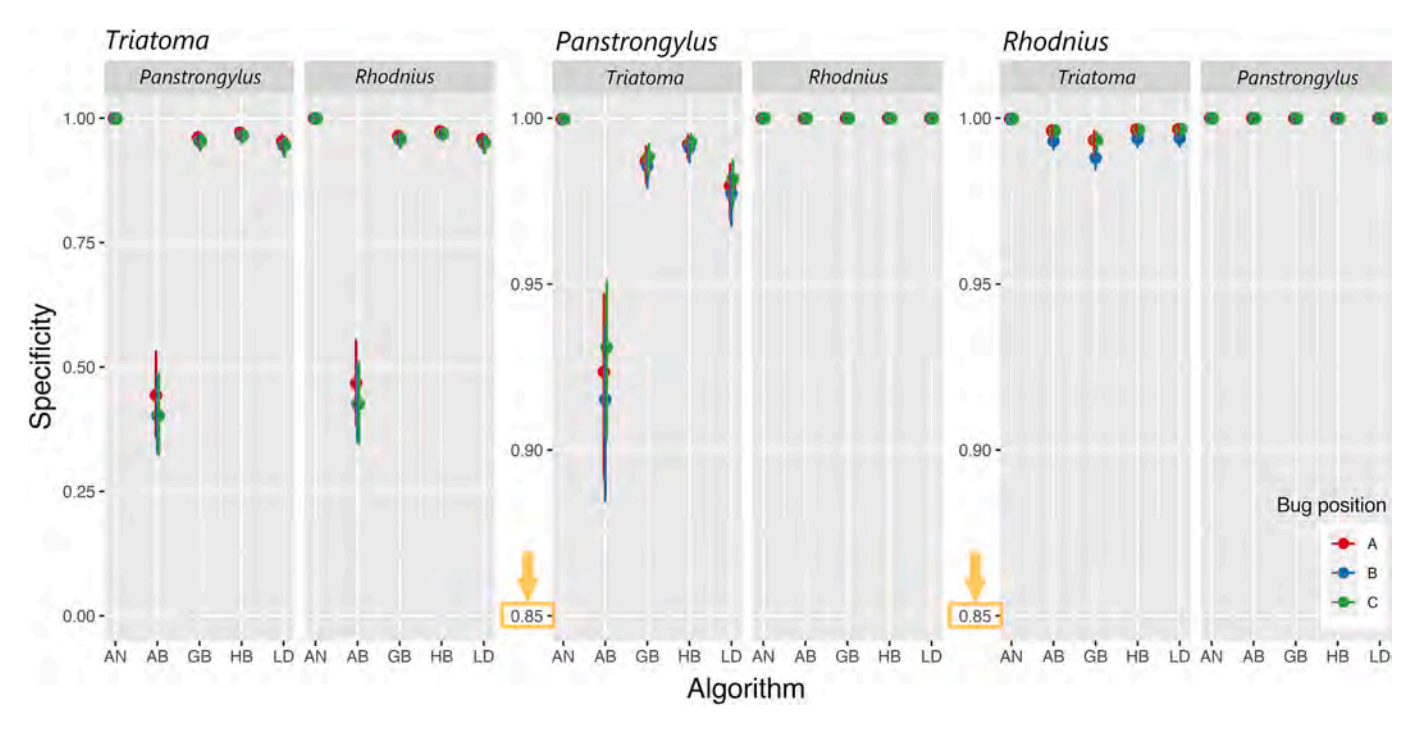


Fig. 6. Cellphone picture-based automated identification of Chagas disease vectors: predictions (with 95% confidence intervals) of the top-ranking generalized linear mixed models for specificity (see Table 3 and Supplementary Tables S10–S12). Predictions are presented for three triatomine bug genera (*Triatoma*, *Panstrongylus*, and *Rhodnius*), five algorithms (AN, AlexNet; AB, AdaBoost Adaptive Boosting; GB, Gradient Boosting; HB, Histogram-based Gradient Boosting; and LD, linear discriminant model), and three bug positions (A, dorsal-flat; B, dorsal-oblique; C, front/back oblique; see Fig. 1). The orange boxes and arrows highlight the different scales of the y-axes (starting at 0.85 instead of at 0.00) in the center and right panels. The data underlying this figure are provided in Supplementary Tables S13–S15.

(e.g., Terry et al., 2020) when trained and tested on non-standardized pictures sourced from field research or citizen-science initiatives. When trained and tested on better-quality pictures (e.g., high-resolution pictures of well-lit whole specimens), artificial neural networks can be even more accurate at identifying, for example, triatomine bugs (Abdelghani et al., 2021; Gurgel-Gonçalves et al., 2017; Khalighifar et al., 2019), mosquitoes (Motta et al., 2020), or ticks (Justen et al., 2021). Because real-world 'extended' (or 'hybrid') surveillance systems will have to rely on pictures of varying quality, most likely taken with cellphone cameras, automated-identification systems that perform well when trained and tested on low-resolution, non-standardized pictures will be critical to advancing the field; our results lend further support to the view that pre-trained artificial neural networks are strong candidates for the role (Cochero et al., 2022; Justen et al., 2021; Motta et al., 2019; Pataki et al., 2021).

It is important to note that the excellent performance of AN that we report (Figs. 2, 3; Supplementary Tables S1, S5, and S6) refers to a relatively simple, three-class (i.e., three-genus) problem. For any given algorithm and picture quality, identification tends to become more challenging as the number of classes increases - e.g., when the task involves many classes (e.g., Khalighifar et al., 2019) instead of just two (e. g., Cochero et al., 2022) or three classes (e.g., Cruz et al., 2021 and this report). In our previous work, the accuracy of two artificial neural networks rose from $\sim\!80\text{--}87\%$ to $\sim\!96\text{--}99\%$ when the number of classes was reduced from 12-39 species to subsets of 2-12 candidate species, with subsetting based on distributional patterns (Khalighifar et al., 2019). While this 'faunal subsetting' approach may help improve the accuracy of automated-identification systems, defining subsets based on known or modeled distributions of species is not without potential pitfalls. Most obviously, species-occurrence records are incomplete and may be biased because of, e.g., uneven sampling effort or false-positive records (Ceccarelli et al., 2018, 2022; Johnston et al., 2023), Perhaps less obviously, methodological challenges inherent in modeling presence records mean that model-predicted distributional summaries should be approached with caution (Araujo et al., 2019; Elith et al.,

2006; Hallgren et al., 2019; Owens et al., 2013; Valavi et al., 2022).

Also importantly, humans have historically introduced several triatomine species well outside of their natural ranges (Monteiro et al., 2018). Because introductions may go undetected for long periods, particularly when surveillance is weak (Abad-Franch et al., 2014), defining a realistic subset of the triatomine fauna likely to be present at any given location and time-point may not be easy; notably, the procedure will by default exclude non-native species, which are often those better adapted to living in human habitats and, hence, the most dangerous vectors of human Chagas disease and top priority for control and surveillance (Abad-Franch, 2016; Gürtler et al., 2021). Careful 'faunal subsetting', in any case, clearly has a major role to play in both 'classical' (e.g., Ribeiro-Jr et al., 2021) and 'extended' vector surveillance, in which accurate automated identification of the 150+ known triatomine-bug species, including some cryptic and some highly variable taxa (Monteiro et al., 2018), may well prove unfeasible without some kind of subsetting (Khalighifar et al., 2019). In general, reliable specimen-specific metadata (on, e.g., collection sites and dates) can be expected to improve the accuracy of automated identification systems (Terry et al., 2020).

Our report also illustrates a mixed model-based approach to evaluating the performance of automated identification systems while taking data dependencies into account (Bolker et al., 2009; Harrison et al., 2018; see also Gurgel-Gonçalves et al., 2021). In our case and in many similar studies, a large number of observations (here, individual outcomes of 65,700 identification tasks) arose from repeatedly using a much smaller number of unique pictures (here, 6570) featuring a much smaller number of unique specimens (here, 730 individual bugs), often across multiple training-testing runs (here, 10 runs) completed by several algorithms (here, five algorithms). Thus, for example, we used picture 'Plutzix10y0' (a dorsal-flat picture of a *Panstrongylus lutzi* specimen) 15 times (in three (pseudo-)replicate runs), and the bug featured in that picture ('Plutzi_10') contributed 85 observations (over all (pseudo-)replicates) to the full dataset (see Supplementary Dataset S1). Those 85 results are not mutually independent, and the random-effects

structure of our accuracy models takes these underlying dependencies into account (Harrison et al., 2018). GLMMs also provide insight into the magnitude of random variation across grouping factors; in our case, for example, accuracy was much more consistent across (pseudo-)replicate runs than it was across specimens or pictures (see Supplementary Table S9). While this analytical approach is a strength of our report, it also highlights a limitation of some of our models. In particular, convergence issues (likely related to high correct-identification frequencies across strata) forced us to drop the 'picture-within-bug' nested random effect in specificity models (see Table 3, Fig. 5, and Supplementary Table S9). As explained in the Methods section and mentioned in the Results section, this simplification means that the output of those models must be interpreted with some caution.

Finally, we note that our Bayesian approach to model fitting relied on choosing what we regard as reasonable prior distributions for model parameters: weakly informative N(0, 9) priors for the fixed effects and flat covariance priors for the random effects (Bolker, 2018; Dorie et al., 2022). To check whether our conclusions were robust to these prior choices, we refit each of the four top-ranking models (Tables 2 and 3, Figs. 4 and 6, and Supplementary Tables S7, S8, and S10–S15) with the following alternative prior specifications: (i) fixed effects: N(0, 14) and N(0, 2.5); and (ii) random effects: Wishart (the default in blme; Dorie et al., 2022; see also Chung et al., 2015), gamma(shape = 2.5, rate = 0) (the default gamma specification in blme; Dorie et al., 2022), and gamma (shape = 2.5, rate = 0.5). The results were closely similar to those reported above and highly robust, with only slight numerical differences, across all comparisons (see Supplementary Figs. S1–S4).

5. Conclusions and outlook

Automated identification of Chagas disease vectors has the potential to strengthen entomological surveillance systems - which are currently weak, and overall getting weaker, across Latin America. To realize such potential fully, automated identification algorithms should be capable of working accurately with pictures of uneven, possibly low quality/resolution taken with ordinary cellphone cameras. Our results suggest that convolutional neural networks may indeed have that capacity, and, hence, that human expertise and artificial intelligence could team up to provide fast, reliable taxonomic support to 'extended' (or 'hybrid'), participatory surveillance systems with broad geographic-ecological scope. However, not all triatomine bug species have the same publichealth relevance, so future research should focus on combining mixedquality pictures and pre-trained neural networks to identify adult triatomine bugs to the species level reliably. Developing automated systems capable of differentiating triatomine nymphs (i.e., immature bug stages, whose presence in or around houses often signals higher risk of disease transmission) from triatomine adults and from other arthropods, including non-blood-feeding bugs, should be seen as another priority. It seems likely that state-of-the-art deep-learning algorithms, such as YOLO (Jiang et al., 2022) and YOLO-based variants (e.g., Roy et al., 2023), will be needed to tackle these more challenging problems, but this remains to be tested empirically. A crucial standing challenge to advancement of these prospects is the need to build 'ground-truth' picture datasets with adequate taxonomic coverage and enough individual specimens (nymphs and adults) to train, validate, and test candidate algorithms robustly. We anticipate that, when fully functional, 'extended' surveillance networks in which well-trained professional staff, mindful citizens, and efficient artificial-intelligence systems all contribute to vector detection, identification, reporting, and mapping, will play critical roles in the sustainable, long-term control of vectorborne diseases including Chagas disease.

Funding

This work was supported by the Coordenação de Aperfeiçoamento de Pessoal de Nível Superior (CAPES, Brazil; Finance Code 001), the Conselho Nacional de Desenvolvimento Científico e Tecnológico (CNPq, Brazil; award numbers 301904/2018-9 and 426619/2018-8), and the US National Science Foundation (NSF, United States of America; award number OIA-1920946).

CRediT authorship contribution statement

Vinícius Lima de Miranda: Conceptualization, Data curation, Formal analysis, Investigation, Methodology, Visualization, Writing – original draft. Ewerton Pacheco de Souza: Investigation, Methodology, Software, Writing – review & editing. Deborah Bambil: Investigation, Methodology, Resources, Software, Writing – review & editing. Ali Khalighifar: Conceptualization, Methodology, Writing – review & editing. A. Townsend Peterson: Conceptualization, Methodology, Writing – review & editing. Francisco Assis de Oliveira Nascimento: Conceptualization, Methodology, Resources, Software, Writing – review & editing. Rodrigo Gurgel-Gonçalves: Conceptualization, Data curation, Funding acquisition, Investigation, Project administration, Supervision, Writing – original draft. Fernando Abad-Franch: Conceptualization, Data curation, Formal analysis, Methodology, Supervision, Validation, Visualization, Writing – original draft, Writing – review & editing.

Declaration of Competing Interest

We have no competing financial interests or personal relationships that could have appeared to influence the work reported in this paper.

Data availability

Triatomine bug pictures used in this study are available on figshare through the following link: https://doi.org/10.6084/m9.figshare.247 86660.v5. The full raw dataset, including picture metadata, is provided in Supplementary Dataset S1.

Acknowledgments

We thank José Roberto Pujol Luz (Universidade de Brasília), Antônio José Camilo Aguiar (Universidade de Brasília), Rita de Cássia Moreira de Souza (Fiocruz Minas Gerais), and Marcos Takashi Obara (Universidade de Brasília) for useful suggestions. The Coordenação de Aperfeiçoamento de Pessoal de Nível Superior (CAPES), Ministério da Educação, Brazil, provides support to the Programa de Pós-graduação em Zoologia at the Universidade de Brasília, Brazil.

Appendix A. Supplementary data

Supplementary data to this article can be found online at https://doi.org/10.1016/j.ecoinf.2023.102430.

References

Abad-Franch, F., 2016. A simple, biologically sound, and potentially useful working classification of Chagas disease vectors. Mem. Inst. Oswaldo Cruz 111. 649-651.

Abad-Franch, F., Monteiro, F.A., Jaramillo, N., Gurgel-Gonçalves, R., Dias, F.B.S., Diotaiuti, L., 2009. Ecology, evolution, and the long-term surveillance of vector-borne Chagas disease: a multi-scale appraisal of the tribe Rhodniini (Triatominae). Acta Trop. 110, 159–177.

Abad-Franch, F., Vega, M.C., Rolon, M.S., Santos, W.S., Rojas de Arias, A., 2011.
Community participation in Chagas disease vector surveillance: systematic review.
PLoS Negl. Trop. Dis. 5. e1207.

Abad-Franch, F., Diotaiuti, L., Gurgel-Gonçalves, R., Gürtler, R.E., 2013. Certifying the interruption of Chagas disease transmission by native vectors: Cui bono? Mem. Inst. Oswaldo Cruz 108, 251–254.

Abad-Franch, F., Diotaiuti, L., Gurgel-Gonçalves, R., Gürtler, R.E., 2014. Reply. On bugs and bias: improving Chagas disease control assessment. Mem. Inst. Oswaldo Cruz 109, 125–130.

Abdelghani, B.A., Banitaan, S., Maleki, M., Mazen, A., 2021. Kissing bugs identification using convolutional neural network. IEEE Access 9, 140539–140548.

- Almeida, A.P.G., Fouque, F., Launois, P., Sousa, C.A., Silveira, H., 2017. From the laboratory to the field: updating capacity building in medical entomology. Trends Parasitol. 33, 664–668.
- Araujo, M.B., Anderson, R.P., Barbosa, A.M., Beale, C.M., Dormann, C.F., Early, R., Garcia, R.A., Guisan, A., Maiorano, L., Rahbek, C., 2019. Standards for distribution models in biodiversity assessments. Sci. Adv. 5, eaat4858.
- Bambil, D., Pistori, H., Bao, F., Weber, V., Alves, F.M., Gonçalves, E.G., Figueiredo, L.F. A., Abreu, U.G.P., Arruda, R., Bortolotto, I.M., 2020. Plant species identification using color learning resources, shape, texture, through machine learning and artificial neural networks. Environ. Syst. Decis. 40, 480–484.
- Bender, A., Python, A., Lindsay, S.W., Golding, N., Moyes, C.L., 2020. Modelling geospatial distributions of the triatomine vectors of *Trypanosoma cruzi* in Latin America. PLoS Negl. Trop. Dis. 14, e0008411.
- Bolker, B.M., 2018. GLMM Worked Examples. Complete separation, Digression. https://bbolker.github.io/mixedmodels-misc/ecostats_chap.html#digression-complete-separation (accessed 19 July 2023).
- Bolker, B.M., Brooks, M.E., Clark, C.J., Geange, S.W., Poulsen, J.R., Stevens, M.H.H., White, J.S.S., 2009. Generalized linear mixed models: a practical guide for ecology and evolution. Trends Ecol. Evol. 24, 127–135.
- Bolker, B.M., R Development Team, Gine-Vazquez, I., 2022. Package 'bbmle'. Tools for general maximum likelihood estimation. https://cran.r-project.org/web/packages/ bbmle/bbmle.pdf (accessed 19 July 2023).
- Burnham, K.P., Anderson, D.R., 2002. Model Selection and Multimodel Inference: A Practical Information-Theoretic Approach, 2nd ed. Springer-Verlag, Berlin.
- Casas, J., Lazzari, C., Insausti, T., Launois, P., Fouque, F., 2016. Mapping of courses on vector biology and vector-borne diseases systems: time for a worldwide effort. Mem. Inst. Oswaldo Cruz 111, 717–719.
- Ceccarelli, S., Balsalobre, A., Medone, P., Cano, M.E., Gurgel-Gonçalves, R., Feliciangeli, D., Vezzani, D., Wisnivesky-Colli, C., Gorla, D.E., Marti, G.A., Rabinovich, J.E., 2018. DataTri, a database of American triatomine species occurrence. Sci. Data 24, 180071.
- Ceccarelli, S., Balsalobre, A., Cano, M.E., Canale, D., Lobbia, P., Stariolo, R., Rabinovich, J.E., Marti, G.A., 2020. Analysis of Chagas disease vectors occurrence data: the Argentinean triatomine species database. Biodiv. Data J. 8, e58076.
- Ceccarelli, S., Balsalobre, A., Vicente, M.E., Curtis-Robles, R., Hamer, S.A., Landa, J.M.A., Rabinovich, J.E., Marti, G.A., 2022. American triatomine species occurrences: updates and novelties in the DataTri database. Gigabyte 2022, gigabyte62.
- Chung, Y., Rabe-Hesketh, S., Dorie, V., Gelman, A., Liu, J., 2013. A nondegenerate penalized likelihood estimator for variance parameters in multilevel models. Psychometrika 78, 685–709.
- Chung, Y., Gelman, A., Rabe-Hesketh, S., Liu, J., Dorie, V., 2015. Weakly informative prior for point estimation of covariance matrices in hierarchical models. J. Educ. Behav. Stat. 40, 136–157.
- Cochero, J., Pattori, L., Balsalobre, A., Ceccarelli, S., Marti, G., 2022. A convolutional neural network to recognize Chagas disease vectors using mobile phone images. Ecol. Inform. 68, 101587.
- Cohen, J., 1960. A coefficient of agreement for nominal scales. Educ. Psychol. Meas. 20, 37–46.
- Cruz, D.D., Arellano, E., Denis Avila, D., Ibarra-Cerdeña, C.N., 2020. Identifying Chagas disease vectors using elliptic Fourier descriptors of body contour: a case for the cryptic dimidiata complex. Parasit. Vectors 13, 332.
- Cruz, D.D., Denis, D., Arellano, E., Ibarra-Cerdeña, C.N., 2021. Quantitative imagery analysis of spot patterns for the three-haplogroup classification of *Triatoma dimidiata* (Latreille, 1811) (Hemiptera: Reduviidae), an important vector of Chagas disease. Parasit. Vectors 14, 90.
- Curtis-Robles, R., Wozniak, E.J., Auckland, L.D., Hamer, G.L., Hamer, S.A., 2015.
 Combining public health education and disease ecology research: using citizen science to assess Chagas disease entomological risk in Texas. PLoS Negl. Trop. Dis. 9, e0004235.
- Dalal, N., Triggs, B., 2005. Histograms of oriented gradients for human detection. In: 2005 IEEE Computer Society Conference on Computer Vision and Pattern Recognition (CVPR'05), San Diego, CA, USA, vol. 1, pp. 886–893.
- Delgado-Noguera, L.A., Hernandez-Pereira, C.E., Ramirez, J.D., Hernandez, C., Velasquez-Ortiz, N., Clavijo, J., Ayala, J.M., Forero-Peña, D., Marquez, M., Suarez, M.J., Traviezo-Valles, L., Escalona, M.A., Perez-Garcia, L., Carpio, I.M., Sordillo, E.M., Grillet, M.E., Llewellyn, M.S., Gabaldón, J.C., Mondolfi, A.E.P., 2022. Tele-entomology and tele-parasitology: a citizen science-based approach for surveillance and control of Chagas disease in Venezuela. Parasite Epidemiol. Control 19, e00273.
- Deniz, O., Bueno, G., Salido, J., de la Torre, F., 2011. Face recognition using histograms of oriented gradients. Pattern Recogn. Lett. 32, 1598–1603.
- Dias, J.C.P., Ramos Jr., A.N., Gontijo, E.D., Luquetti, A., Shikanai-Yasuda, M.A., Coura, J. R., Torres, R.M., Melo, J.R.C., Almeida, E.A., de Oliveira Jr, W., Silveira, A.C., de Rezende, J.M., Pinto, F.S., Ferreira, A.W., Rassi, A., Fragata Filho, A.A., de Sousa, A. S., Correia Filho, D., Jansen, A.M., Andrade, G.M.Q., Britto, C.F.P., Pinto, A.Y.N., Rassi Jr., A., Campos, D.E., Abad-Franch, F., Santos, S.E., Chiari, E., Hasslocher-Moreno, A.M., Moreira, E.F., Marques, D.S.O., Silva, E.L., Marin-Neto, J.A., Galvão, L.M.C., Xavier, S.S., Valente, S.A.S., Carvalho, N.B., Cardoso, A.V., Silva, R. A., da Costa, V.M., Vivaldini, S.M., Oliveira, S.M., Valente, V.C., Lima, M.M., Alves, R., 2016. 2nd Brazilian consensus on Chagas disease, 2015. Rev. Soc. Bras. Med. Trop. 49 (Suppl. 1), 3–60.
- Dorie, V., Bates, D., Maechler, M., Bolker, B., Walker, S., 2022. Package 'blme'. Bayesian linear mixed-effects models. https://cran.r-project.org/web/packages/blme/blme.pdf (accessed 19 July 2023).
- Elith, J., Graham, C.H., Anderson, R.P., Dudik, M., Ferrier, S., Guisan, A., Hijmans, R.J., Huettmann, F., Leathwick, J.R., Lehmann, A., Li, J., Lohmann, L.G., Loiselle, B.A.,

- Manion, G., Moritz, C., Nakamura, M., Nakazawa, Y., Overton, J.M.M., Peterson, A. T., Phillips, S.J., Richardson, K., Scachetti-Pereira, R., Schapire, R.E., Soberón, J., Williams, S., Wisz, M.S., Zimmermann, N.E., 2006. Novel methods improve prediction of species' distributions from occurrence data. Ecography 29, 129–151.
- Fisher, R.A., 1936. The use of multiple measurements in taxonomic problems. Ann. Eugenics 7, 179–188.
- Flusser, J., Zitova, B., Suk, T., 2009. Moments and Moment Invariants in Pattern Recognition. Wiley, New York.
- Freund, Y., Schapire, R.E., 1997. A decision-theoretic generalization of on-line learning and an application to boosting. J. Comput. Syst. Sci. 55, 119–139.
- Friedman, J.H., 2001. Greedy function approximation: a gradient boosting machine. Ann. Stat. 29, 1189–1232.
- Galvão, C. (Org.), 2014. Vetores da Doença de Chagas no Brasil. Sociedade Brasileira de Zoologia, Curitiba.
- GBD Global Burden of Disease Collaborative Network, 2019. Global Burden of Disease Study 2019 (GBD 2019) Results. Institute for Health Metrics and Evaluation, Seattle. http://ghdx.healthdata.org/gbd-results-tool (accessed 5 July 2023).
- Gorla, D.E., 2002. Variables ambientales registradas por sensores remotos como indicadores de la distribución geográfica de *Triatoma infestans* (Heteroptera: Reduviidae). Ecol. Austral 12, 117–127.
- Gurgel-Gonçalves, R., 2022. Stronger control-surveillance systems for vector-borne Chagas disease. Mem. Inst. Oswaldo Cruz 117 e210130chgsb.
- Gurgel-Gonçalves, R., Galvão, C., Costa, J., Peterson, A.T., 2012. Geographic distribution of Chagas disease vectors in Brazil based on ecological niche modeling. J. Trop. Med. 2012. 705326.
- Gurgel-Gonçalves, R., Komp, E., Campbell, L.P., Khalighifar, A., Mellenbruch, J., Mendonça, V.J., Owens, H.L., Felix, K.C., Peterson, A.T., Ramsey, J.M., 2017. Automated identification of insect vectors of Chagas disease in Brazil and Mexico: the Virtual Vector Lab. PeerJ 5, e3040.
- Gurgel-Gonçalves, R., Abad-Franch, F., de Almeida, M.R., Obara, M.T., de Souza, R.C.M., Batista, J.A.D.S., Rocha, D.D.A., 2021. TriatoDex, an electronic identification key to the Triatominae (Hemiptera: Reduviidae), vectors of Chagas disease: development, description, and performance. PLoS One 16, e0248628.
- Gürtler, R.E., Cecere, M.C., 2021. Chagas disease vector control. In: Guarneri, A.A.,
 Lorenzo, M.G. (Eds.), Triatominae: The Biology of Chagas Disease Vectors,
 Entomology in Focus, vol. 5. Springer, Cham, pp. 491–535.
 Gürtler, R.E., Fernández, M.P., Cardinal, M.V., 2021. Eco-epidemiology of vector-borne
- Gürtler, R.E., Fernández, M.P., Cardinal, M.V., 2021. Eco-epidemiology of vector-borne transmission of *Trypanosoma cruzi* in domestic habitats. In: Guarneri, A.A., Lorenzo, M.G. (Eds.), Triatominae: The Biology of Chagas Disease Vectors. Entomology in Focus, vol. 5. Springer, Cham, pp. 447–489.
- Hallgren, W., Santana, F., Low-Choy, S., Zhao, Y., Mackey, B., 2019. Species distribution models can be highly sensitive to algorithm configuration. Ecol. Model. 408, 108719.
- Hamer, S.A., Curtis-Robles, R., Hamer, G.L., 2018. Contributions of citizen scientists to arthropod vector data in the age of digital epidemiology. Curr. Opin. Insect Sci. 28, 98-104
- Harrel, F., Dupont, C., 2023. Package 'Hmisc': Harrell miscellaneous. https://cran.r-project.org/web/packages/Hmisc/Hmisc.pdf (accessed 19 July 2023).
- Harrison, X.A., Donaldson, L., Correa-Cano, M.E., Evans, J., Fisher, D.N., Goodwin, C.E., Robinson, B.S., Hodgson, D.J., Inger, R., 2018. A brief introduction to mixed effects modelling and multi-model inference in ecology. PeerJ 6, e4794.
- Hashimoto, K., Zuniga, C., Romero, E., Morales, Z., Maguire, J.H., 2015. Determinants of health service responsiveness in community-based vector surveillance for Chagas disease in Guatemala, El Salvador, and Honduras. PLoS Negl. Trop. Dis. 9, e0003974.
- Hu, M.-K., 1962. Visual pattern recognition by moment invariants. IRE Trans. Inf. Theory 8, 179–187.
- Jansen, A.M., Roque, A.L.R., 2010. Domestic and wild mammalian reservoirs. In: Telleria, J., Tibayrenc, M. (Eds.), American Trypanosomiasis (Chagas Disease): One Hundred Years of Research. Elsevier, London, pp. 249–276.
- Jiang, P., Ergu, D., Liu, F., Cai, Y., Ma, B., 2022. A review of Yolo algorithm developments. Procedia Comput. Sci. 199, 1066–1073.
- Johnston, A., Matechou, E., Dennis, E.B., 2023. Outstanding challenges and future directions for biodiversity monitoring using citizen science data. Methods Ecol. Evol. 14, 103–116.
- Justen, L., Carlsmith, D., Paskewitz, S.M., Bartholomay, L.C., Bron, G.M., 2021.
 Identification of public submitted tick images: a neural network approach. PLoS One 16, e0260622.
- Khalighifar, A., Komp, E., Ramsey, J.M., Gurgel-Gonçalves, R., Peterson, A.T., 2019. Deep learning algorithms improve automated identification of Chagas disease vectors. J. Med. Entomol. 56, 1404–1410.
- Krizhevsky, A., Sutskever, I., Hinton, G.E., 2012. ImageNet classification with deep convolutional neural networks. Adv. Neural Inf. Process. Sys. 25, 1106–1114.
- Leite, G.R., dos Santos, C.B., Falqueto, A., 2011. Influence of the landscape on dispersal of sylvatic triatomines to anthropic habitats in the Atlantic Forest. J. Biogeogr. 38, 651–663.
- Lent, H., Wygodzinsky, P., 1979. Revision of the Triatominae (Hemiptera, Reduviidae), and their significance as vectors of Chagas' disease. Bull. Am. Mus. Nat. Hist. 163, 123–520.
- Marsden, P.D., 1984. Selective primary health care: strategies for control of disease in the developing world. XVI. Chagas' disease. Rev. Infect. Dis. 6, 855–865.
- Miranda, V.L., Souza, E.P., Bambil, D., Khalighifar, A., Peterson, A.T., Nascimento, F.A. O., Gurgel-Gonçalves, R., Abad-Franch, F., 2023. Triatomine bug pictures from "Cellphone picture-based, genus-level automated identification of Chagas disease vectors: effects of picture orientation on the performance of five machine-learning algorithms". Figshare https://doi.org/10.6084/m9.figshare.24786660.v5.

- Monteiro, F.A., Weirauch, C., Felix, M., Lazoski, C., Abad-Franch, F., 2018. Evolution, systematics, and biogeography of the Triatominae, vectors of Chagas disease. Adv. Parasitol. 99, 265–344.
- Motta, D., Santos, A.A.B., Winkler, I., Machado, B.A.S., Pereira, D.A.D.I., Cavalcanti, A. M., Fonseca, E.O.L., Kirchner, F., Badaro, R., 2019. Application of convolutional neural networks for classification of adult mosquitoes in the field. PLoS One 14, e0210829.
- Motta, D., Santos, A.A.B., Machado, B.A.S., Ribeiro-Filho, O.G.V., Camargo, L.O.A., Valdenegro-Toro, M.A., Kirchner, F., Badaro, R., 2020. Optimization of convolutional neural network hyperparameters for automatic classification of adult mosquitoes. PLoS One 15, e0234959.
- Nascimento, F.A.O., Saraiva Jr., R.G., Faria, E.G.C., Silva, T.A.M., Carvalho, J.L.A., 2023. Computational intelligence conceptions to automated diagnosis: feature grouping for performance improvement. Braz. Arch. Biol. Technol. 66, e23230609.
- Newcombe, R.G., 1998. Two-sided confidence intervals for the single proportion: comparison of seven methods. Stat. Med. 17, 857–872.
- Oliveira, M.L., Brito, R.N., Guimarães, P.A.S., dos Santos, R.V.M.A., Diotaiuti, L.G., Souza, R.C.M., Ruiz, J.C., 2017. TriatoKey: a web and mobile tool for biodiversity identification of Brazilian triatomine species. Database 2017, bax033.
- Owens, H.L., Campbell, L.P., Dornak, L.L., Saupe, E.E., Barve, N., Soberón, J., Ingenloff, K., Lira-Noriega, A., Hensz, C.M., Myers, C.E., Peterson, A.T., 2013. Constraints on interpretation of ecological niche models by limited environmental ranges on calibration areas. Ecol. Model. 263, 10–18.
- Park, J., Kim, D.I., Choi, B., Kang, W., Kwon, H.W., 2020. Classification and morphological analysis of vector mosquitoes using deep convolutional neural networks. Sci. Rep. 10, 1012.
- Parsons, Z., Banitaan, S., 2021. Automatic identification of Chagas disease vectors using data mining and deep learning techniques. Ecol. Inform. 62, 101270.
- Pataki, B.A., Garriga, J., Eritja, R., Palmer, J.R.B., Bartumeus, F., Csabai, I., 2021. Deep learning identification for citizen science surveillance of tiger mosquitoes. Sci. Rep. 11, 4718.
- Pedregosa, F., Varoquaux, G., Gramfort, A., Michel, V., Thirion, B., Grisel, O., Blondel, M., Prettenhofer, P., Weiss, R., Dubourg, V., Vanderplas, J., Passos, A., Cournapeau, D., Duchesnay, E., 2011. Scikit-learn: machine learning in Python. J. Mach. Learn. Res. 12, 2825–2830.
- Pérez-Molina, J.A., Molina, I., 2018. Chagas disease. Lancet 391, 82-94.
- Posit Software, 2022. RStudio 2023.03.1.446. https://posit.co/products/open-source/rstudio/.
- Prata, A., 2001. Clinical and epidemiological aspects of Chagas disease. Lancet Infect. Dis. 1, 92–100.
- R Core Team, 2022. R: A Language and Environment for Statistical Computing. The R Foundation for Statistical Computing. https://www.R-project.org/.

- Ribeiro-Jr, G., Abad-Franch, F., de Sousa, O.M., Dos Santos, C.G., Fonseca, E.O., dos Santos, R.F., Cunha, G.M., de Carvalho, C.M.M., Reis, R.B., Gurgel-Gonçalves, R., Reis, M.G., 2021. TriatoScore: an entomological-risk score for Chagas disease vector control-surveillance. Parasit. Vectors 14, 492.
- Rojas de Arias, A., Monroy, C., Guhl, F., Sosa-Estani, S., Santos, W.S., Abad-Franch, F., 2022. Chagas disease control-surveillance in the Americas: the multinational initiatives and the practical impossibility of interrupting vector-borne *Trypanosoma cruzi* transmission. Mem. Inst. Oswaldo Cruz 117, e210130.
- Roy, A.M., Bhaduri, J., Kumar, T., Raj, K., 2023. WilDect-YOLO: an efficient and robust computer vision-based accurate object localization model for automated endangered wildlife detection. Ecol. Inform. 75, 101919.
- Schofield, C.J., Jannin, J., Salvatella, R., 2006. The future of Chagas disease control. Trends Parasitol. 22, 583–588.
- Silveira, A.C., Feitosa, V.R., Borges, R., 1984. Distribuição de triatomíneos capturados no ambiente domiciliar, no período 1975/83, Brasil. Rev. Bras. Malariol. Doencas Trop. 36, 15–312.
- Terry, J.C.D., Roy, H.E., August, T.A., 2020. Thinking like a naturalist: enhancing computer vision of citizen science images by harnessing contextual data. Methods Ecol. Evol. 11, 303–315.
- Tharwat, A., Gaber, T., Ibrahim, A., Hassanien, A.E., 2017. Linear discriminant analysis: a detailed tutorial. AI Commun. 30, 169–190.
- Valavi, R., Guillera-Arroita, G., Lahoz-Monfort, J.J., Elith, J., 2022. Predictive performance of presence-only species distribution models: a benchmark study with reproducible code. Ecol. Monogr. 92, e01486.
- Vinhaes, M.C., de Oliveira, S.V., Reis, P.O., de Lacerda Sousa, A.C., Albuquerque, R., Obara, M.T., Bezerra, C.M., Costa, V.M., Alves, R.V., Gurgel-Gonçalves, R., 2014. Assessing the vulnerability of Brazilian municipalities to the vectorial transmission of *Trypanosoma cruzi* using multi-criteria decision analysis. Acta Trop. 137, 105–110.
- WHO World Health Organization, 2002. Control of Chagas disease: second report of the WHO Expert Committee. WHO Tech. Rep. Ser. 905, 1–109.
- WHO World Health Organization, 2017. Global vector control response 2017–2030. World Health Organization, Geneva.
- Yadon, Z., Gürtler, R.E., Tobar, F., Medici, A.C. (Eds.), 2006. Descentralización y Gestión del Control de Enfermedades Transmisibles en América Latina. PAHO/WHO, Buenos Aires.
- Yoshioka, K., Tercero, D., Pérez, B., Nakamura, J., Perez, L., 2017. Implementing a vector surveillance-response system for Chagas disease control: a 4-year field trial in Nicaragua. Infect. Dis. Poverty 6, 18.
- Zhao, G., Pietikainen, M., 2007. Dynamic texture recognition using local binary patterns with an application to facial expressions. IEEE Trans. Pattern Anal. Mach. Intell. 29, 915–928.